

Initial-state parton shower kinematics for NLO event generators

Shigeru Odaka ^a and Yoshimasa Kurihara

High Energy Accelerator Research Organization (KEK), 1-1 Oho, Tsukuba, Ibaraki 305-0801, Japan

Received: date / Revised version: date

Abstract. We are developing NLO event generators for hadron collision interactions based on the limited leading-log (LLL) subtraction method. In this method, a boundary between non-radiative and radiative processes necessarily appears at the factorization scale (μ_F). The radiation effects are simulated using a parton shower (PS) in non-radiative processes. It is therefore crucial in our method to apply a PS which well reproduces the radiation activities evaluated from the matrix-element (ME) calculations for radiative processes. The PS activity depends on the applied kinematics model. In this paper we introduce two models for our simple initial-state leading-log PS: a model similar to the "old" PYTHIA-PS and a p_T -prefixed model with a p_T definition motivated by ME calculations. PS simulations employing these models are tested using W -boson production at LHC as an example. Both simulations show a smooth matching to the LLL-subtracted $W + 1$ jet simulation in the p_T distribution of W bosons, and the summed p_T spectra are stable against a variation of μ_F , despite that the p_T -prefixed PS results in an apparently harder p_T spectrum than the PS with the "old" PYTHIA-like kinematics. The "new" PYTHIA-PS gives a transverse activity similar to our p_T -prefixed PS. The choice of the model has to be postponed to further studies employing a comparison with experimental data.

arXiv:hep-ph/0702138v1 14 Feb 2007

^a E-mail: shigeru.odaka@kek.jp

1 Introduction

Next-to-leading order (NLO) corrections are necessary to derive theoretically consistent predictions in Quantum Chromodynamics (QCD), and are required by experiments for precise measurements of known processes and reliable estimates of the background for expected heavy particle productions at high-energy hadron collisions, such as those at Fermilab Tevatron and the forthcoming CERN LHC. The corrections are desired to be implemented in Monte-Carlo event generators for the latter use because they may depend on the topology of the events experimentally selected.

The implementation of NLO corrections in event generators, in general, has a problem in regularizing the collinear and soft divergences; *i.e.*, the cancellation of divergences in radiative processes and non-radiative processes. Phase-space slicing methods that are usually applied in electroweak corrections are problematic for QCD corrections because of the large coupling. They frequently lead to large negative cross sections in non-radiative processes and/or visible boundaries in the phase space of radiative processes. The former severely ruins the usability of event generators, and the latter is undesirable for use in experimental analyses.

For estimating interactions at high-energy hadron collisions, it is also necessary to employ an appropriate parton distribution function (PDF) and fragmentation functions (FF), depending on the energy scale of the perturbatively evaluated hard interaction. They resum large logarithmic collinear corrections to all orders to improve the convergence of the perturbation. These collinear corrections are usually simulated in event generators in the form of a parton shower (PS), because experiments require an exclusive simulation of beam collisions, and the corrections produce an experimentally visible transverse boost of the hard interaction and additional hadron activities. The corrections by PDF, FF and PS have an apparent overlap with NLO corrections based on matrix-element (ME) calculations. We have to avoid double counts in order to construct consistent NLO event generators.

Subtraction methods [1,2] naturally solve these problems, in which the divergent terms are subtracted from radiative processes and their integrated contributions are added to non-radiative processes. The emergence of negative cross sections is limited and all results become finite, since the divergences are canceled within non-radiative processes. The application of PDF/FF and/or PS automatically restores the corrections, if the subtracted terms are identical to their leading contributions. The concept is simple, while implementation in event generators is not easy because the matching between the subtraction and the actual PS implementation is not trivial. After many trials, a practical solution [3] has been presented based on detailed knowledge on the initial-state PS of HERWIG [4], and has been applied to several color-singlet production and heavy-flavor production processes where it is enough to consider radiations from initial-state partons. Recently, a new idea has been proposed to make the cross sections totally positive [5].

We are developing NLO event generators based on a different concept of subtraction [6]. Our goal is to develop an automated generation system of NLO event generators for hadron collision interactions based on GRACE [7]. We adopt a leading-log (LL) subtraction method so as to avoid large negative cross sections and double counts, where a naive LL approximation to the parton radiation, proportional to $1/Q^2$, is subtracted from radiative processes. Though the implementation is still limited to the initial-state radiation, extension to the final state will be easy since the concept is quite simple.

In our method, radiative processes simulate the hard LL part, harder than the factorization scale (μ_F), and the non-LL part of the radiation. The softer LL part is simulated by the PS applied to non-radiative processes. Therefore, it is crucial in this method to employ a PS that well matches with the ME calculation of the radiation. In order to make the discussions transparent, we have developed an initial-state PS that strictly reproduces theoretical arguments in the LL approximation. A primary feasibility of this method has been demonstrated in a previous paper [6]. The theoretical arguments are, however, performed only at the collinear limit. We need to introduce an appropriate kinematics model in order to construct a PS that is usable in practical event generators. The model applied in the demonstration was very primitive.

In the present study we introduce two practical models of the PS kinematics and examine their matching properties, using W -boson production at the LHC condition as an example. Since this process has an apparent fixed energy scale of the W -boson mass (m_W), possible mismatches would become visible in physical distributions. The matching can be tested without introducing loop corrections. The tests are carried out in the present study by using simulations employing tree-level ME calculations of the inclusive W ($W + 0$ jet) and $W + 1$ jet production processes, where "jet" denotes a light quark or gluon in the final state. We examine only the internal consistency of our method. Comparison with experimental data will be done in a separate paper, where additional lower Q^2 effects, such as the intrinsic p_T and the underlying events, must be taken into account.

This paper is organized as follows: the bases of our LL-PS and the LL subtraction are given in Section 2. The description includes some details of the LL subtraction for the sample process. The kinematics models are introduced and tested in Sections 3 and 4. Finally, the conclusion is presented in Section 5.

2 Parton Shower and LL subtraction

We use an x -deterministic forward evolution [6] for the initial-state PS. This technique is a solution to overcome the low-efficiency problem in the forward evolution. Starting from a small Q^2 , the PS strictly reproduces the QCD evolution implemented in PDFs. The final Bjorken's x is thus given by the PS. The PS energy scale (μ_{PS}), the maximum energy scale in PS, is therefore necessarily identical to the factorization scale (μ_F), the energy scale of PDF. This means that the PS radiation is limited by μ_F . The limitation is taken into account in the subtraction as well. Hereafter, we call this technique the limited leading-log (LLL) subtraction.

In our PS we refer to a PDF at a low energy scale ($Q_0 = 4.6$ GeV) and produce branches in increasing order of Q^2 until reaching $Q^2 = \mu_F^2$. The Q^2 of each branch is determined according to the Sudakov form factor, expressed as

$$S(Q_1^2, Q_2^2) = \exp \left[- \int_{Q_1^2}^{Q_2^2} \frac{dQ^2}{Q^2} \int_{\epsilon}^{1-\epsilon} dz \frac{\alpha_s(Q^2)}{2\pi} P(z) \right], \quad (1)$$

where $P(z)$ is the Altarelli-Parisi splitting function at the leading order;

$$P(z)_{q \rightarrow qg} = C_F \frac{1+z^2}{1-z}, \quad (2)$$

$$P(z)_{g \rightarrow gg} = N_C \frac{(1-z(1-z))^2}{z(1-z)}, \quad (3)$$

$$P(z)_{g \rightarrow q\bar{q}} = T_R(z^2 + (1-z)^2), \quad (4)$$

for the branches $q \rightarrow qg$, $g \rightarrow gg$ and $g \rightarrow q\bar{q}$, respectively, with $C_F = 4/3$, $N_C = 3$ and $T_R = n_f/2 = 5/2$. The splitting function $P(z)$ is summed over possible branches. We use CTEQ5L [10] for the reference PDF in the present study. Accordingly we use the first-order strong coupling,

$$\alpha_s(Q^2) = \frac{4\pi}{\beta_0 \ln(Q^2/\Lambda^2)} \quad (5)$$

with $\beta_0 = 11 - 2n_f/3$ and $\Lambda = 0.146$ GeV for $n_f = 5$. The branching mode and the parameter z are determined in proportion to $P(z)$ of relevant branches. An unphysical parameter, ϵ , is introduced in order to cutoff the divergence of $P(z)$. We set $\epsilon = 10^{-6}$ as the default. Physical properties do not depend on this choice if ϵ is set to be sufficiently small.

PS is a Monte-Carlo solution of the QCD evolution based on the factorization theory. In this theory, the evolution is considered at the collinear limit in an infinite-momentum frame. The transverse behavior of the radiation is given only at the first-order approximation. As a result, the predicted kinematics do not strictly conserve the energy and momentum. We therefore need to introduce a certain model of the branching kinematics that gives a correspondence of the above branching parameters, Q^2 and z , to kinematical variables in a finite-momentum frame, to construct a practical PS strictly conserving the energy and momentum. The purpose of this paper is to introduce such models and test their feasibility in our subtraction method.

Though the LL subtraction is not a main subject of this paper, we here describe some details for the present example process, $W + 1$ jet production, since it is used for the tests of PS models in the following sections. At the parton level, the $W + 1$ jet production process is composed of three incoherent subprocesses:

$$q\bar{q}' \rightarrow gW, \quad (6)$$

$$g\bar{q}' \rightarrow qW, \quad (7)$$

$$qg \rightarrow q'W. \quad (8)$$

We ignore CKM nondiagonal interactions in the present study. Therefore, (q, q') denotes (d, u) , (u, d) , (s, c) or (c, s) .

The W bosons are assumed to decay to a pair of an electron and a neutrino. The matrix elements are evaluated including this decay at the tree level, assuming a total decay width of 2.12 GeV. The

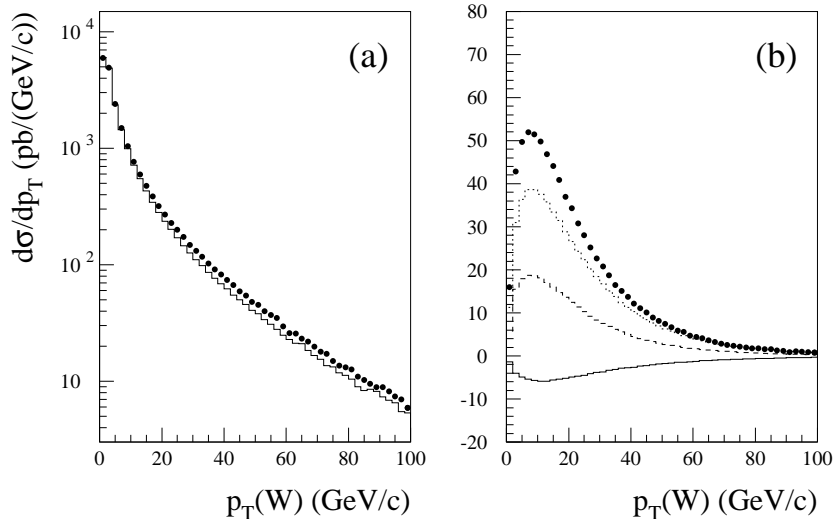


Fig. 1. $W + 1$ jet cross section at LHC as a function of the W -boson p_T : (a) the sum of three incoherent subprocesses, and (b) the residual of the LL subtraction. A p_T cut of 1 GeV/ c is applied, while PS is yet to be applied in these results. The result from exact matrix elements at the tree level (filled circles) is compared with that from the LL approximation (histogram) in (a). The result is shown for each subprocess, $q\bar{q}' \rightarrow gW$ (solid), $g\bar{q}' \rightarrow qW$ (dashed), and $qg \rightarrow q'W$ (dotted), separately in (b), together with the sum shown with filled circles.

calculations are performed within the framework of BASES/SPRING [8] employing the matrix-element codes generated by GRACE [7]. The studies in this paper are carried out using cross-section results from BASES. The same method is applied for simulating the inclusive W ($W + 0$ jet) production, too.

Subtraction is done at the matrix-element level as [6]

$$|\mathcal{M}_{\text{LLsub}}(\hat{s}; \mu_R)|^2 = |\mathcal{M}_{W+j}(\hat{s}; \mu_R)|^2 - |\mathcal{M}_W(\hat{s}_W)|^2 f_{\text{LL}}(x, t; \mu_R), \quad (9)$$

where \mathcal{M}_{W+j} is the matrix element for a given $W + 1$ jet event with a squared center-of-mass (cm) energy of \hat{s} , and \mathcal{M}_W is that for the W production sub-system in this event having a squared invariant mass of \hat{s}_W . The rotation of the sub-system is also taken into account in the calculation, though it is irrelevant to the following studies since the angular properties are always integrated. The LL radiation factor f_{LL} can be written as

$$f_{\text{LL}}(x, t; \mu_R) = \frac{\alpha_s(\mu_R^2)}{2\pi} \frac{P(x)}{x} \frac{16\pi^2}{|t|}, \quad (10)$$

where $P(x)$ is an Altarelli-Parisi splitting function relevant to this event. It is essential to use an identical definition of α_s in the $W + 1$ jet matrix element \mathcal{M}_{W+j} and in the LL factor f_{LL} . We use the definition of Eq. (5) with the energy scale Q^2 set to a fixed value (μ_R^2) in the present study.

The parameter x is the ratio of the squared cm energies ($x = \hat{s}_W/\hat{s}$), and t is the squared momentum transfer of the parton branch in the picture of PS. There are two possibilities in the definition of t for the subprocess (6). The gluon in the final state can be radiated from q and \bar{q}' in the initial state. We have to subtract both contributions. Thus, t is defined using the four-momenta of the partons as $1/|t| = 1/|t_q| + 1/|t_{q'}|$ with $t_q = (p_q - p_g)^2$ and $t_{q'} = (p_{q'} - p_g)^2$. On the other hand, there is no ambiguity for subprocesses (7) and (8), since $g \rightarrow q\bar{q}$ is the unique possible branch. The parameter t is defined as $t = (p_g - p_q)^2$ for (7) and $t = (p_g - p_{q'})^2$ for (8).

The subtraction result at the cross-section level is shown in Fig. 1 as a function of the transverse momentum of the W boson, where PS is yet to be applied. The matrix elements are converted to the cross sections assuming the LHC condition (proton-proton collisions at the cm energy of 14 TeV) and using CTEQ5L for PDF. The renormalization scale μ_R and the factorization scale μ_F are both fixed to the W -boson mass ($m_W = 80.2$ GeV). A p_T cut is necessary to apply since the subtraction is done numerically. We set the minimum p_T to 1 GeV/ c . These conditions are valid throughout the present study, except for the choice of μ_F .

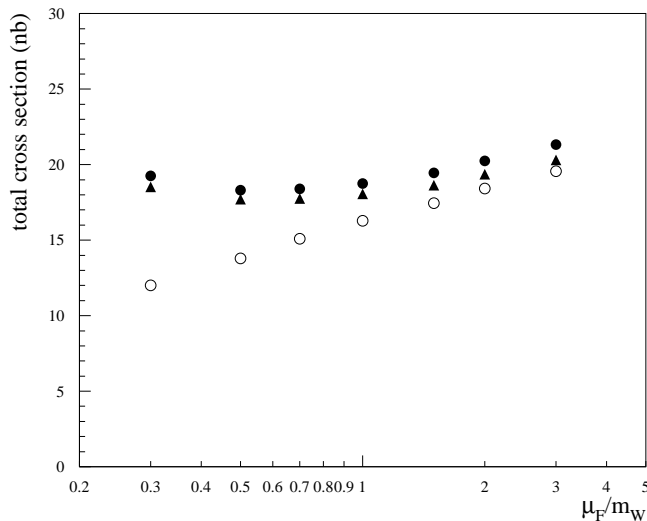


Fig. 2. Factorization scale (μ_F) dependence of the total cross section for W production at LHC. An apparent μ_F dependence in the inclusive W production cross section (open circles) is greatly reduced if the $W + 1$ jet cross section with the LLL (limited LL) subtraction is added (filled circles). Filled triangles illustrate the results from a simulation where the PS employing the p_T -prefixed kinematics model is applied. The cross section result is affected by the PS veto in the $W + 1$ jet simulation. The PDF is slightly changed since the QCD evolution is evaluated by PS in our simulation.

Figure 1(a) shows the cross section based on the exact $W + 1$ jet matrix element (filled circles) and that based on the LL approximation (histogram); *i.e.*, they correspond to the first and the second term in the right-hand side of Eq. (9), respectively. The result from the subtracted matrix element is plotted in Fig. 1(b) with filled circles. The result is also shown for each subprocess separately. The residual is always negative for subprocess (6) and positive for (7) and (8). The sum (filled circles) is positive since the contribution of the subprocess (8) is large in proton-proton collisions. We can see that the residual is going to vanish as p_T goes to zero in all subprocesses, and the small p_T cut does not significantly affect the final results.

In the LLL (limited LL) subtraction, the subtraction is applied only when $|t_q| < \mu_F^2$ or $|t_{q'}| < \mu_F^2$ in the subprocess (6), and when $|t| < \mu_F^2$ in the subprocesses (7) and (8). Here we note that both the $W + 0$ jet and the subtracted $W + 1$ jet cross sections depend on μ_F . The LL contributions of the parton radiation below the energy scale of μ_F are resummed by PDF and PS in the former, while those above μ_F are explicitly evaluated at the first order of α_s in the latter. The non-LL contributions are all remaining in the latter. Thus, we can expect that the dependence on μ_F cancels in the sum of these two cross sections, at least at the leading order of α_s .

The summed total cross section is plotted in Fig. 2 with filled circles as a function of μ_F . They should be compared with the inclusive W production cross section shown with open circles. We can see that the μ_F dependence is greatly reduced in the summed cross section, as we expected. The variation is at most 10% within the range of $1/2 \leq \mu_F/m_W \leq 2$. This is a remarkable feature of the LLL subtraction. The stability will become better if an appropriate resummation (Sudakov suppression) is applied to the $W + 1$ jet process. It will suppress a small enhancement at very small μ_F values in Fig. 2, as demonstrated in a previous paper [9].

3 PYTHIA kinematics

We first test the kinematics model of the "old" PYTHIA-PS for the initial state [12] because this PS is constructed on nearly the same theoretical basis as ours. The starting assumption of this model is that the Q^2 of the evolution is identical to the virtuality of the evolving parton,

$$p_{\text{evol}}^2 = -Q^2, \quad (11)$$

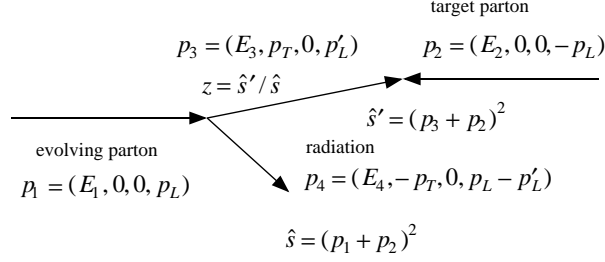


Fig. 3. Definition of kinematical variables in each parton branch. The calculation is done in the cm frame of the evolving parton and the target parton.

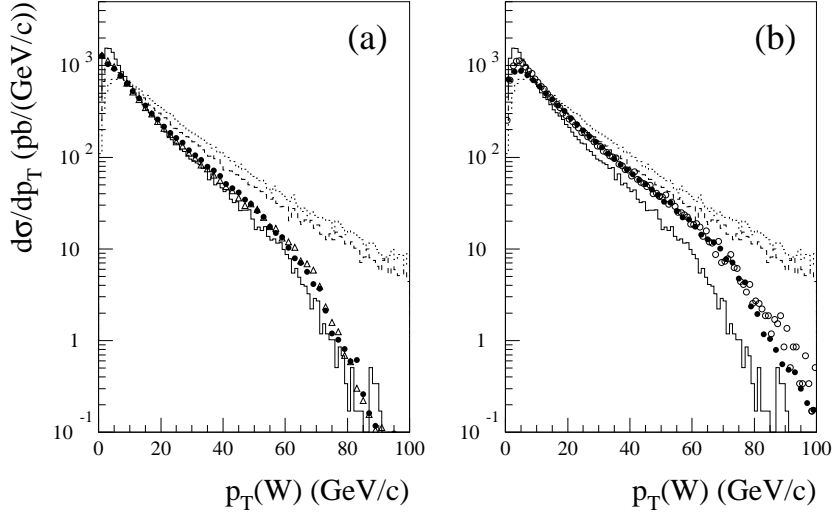


Fig. 4. Simulated transverse momentum (p_T) distribution of W bosons in the inclusive W production process at the LHC condition. Filled circles show the result of our simulation: (a) with the "old" PYTHIA-PS kinematics model and (b) with the p_T -prefixed model. Solid histograms show the result from "old" PYTHIA without the ME correction to the initial-state radiation. The "old" and "new" PYTHIA simulations with the ME correction are illustrated with dashed and dotted histograms, respectively, for reference. Open triangles in (a) show the result of a p_T -prefix model with a non-standard assumption of $p_T^2 = (1-z)^2 Q^2$, and open circles in (b) the result of the "new" PHYTHA simulation without the ME correction.

and z gives the ratio between the squared cm energies after and before a branch,

$$z = \hat{s}' / \hat{s}. \quad (12)$$

The latter ensures the relation $\hat{s}_{\text{hard}} = x_1 x_2 s$ between the squared cm energies of the hard interaction and the beam collision, with x given by the product of all z values in each beam.

The transverse momentum (p_T) of each branch is calculated from energy-momentum conservation conditions [12,9]. The definition of kinematical variables is illustrated in Fig. 3. Assumption (11) leads to $p_3^2 = -Q^2$, while p_1^2 is given by the previous branch. The definition of z requires a target parton. The definition is not trivial since two incoming partons are both evolving. We execute the branches in the increasing order of Q^2 equally taking both sides into consideration. The remaining parton on the opposite side is chosen as the target. Therefore, the target parton is also virtual. Going into further details, the calculation sometimes gives a negative p_T^2 . In such cases we set p_T to zero and adjust the Q^2 to give this solution.

Filled circles in Fig. 4(a) show the simulated p_T distribution of W -bosons in the inclusive W production process for the LHC condition with $\mu_F = m_W$. The corresponding prediction from the "old" PYTHIA-PS is shown with a histogram, where PYTHIA 6.403 [11] is used with $\text{MSTP}(68) = 0, \text{MSTP}(71)$

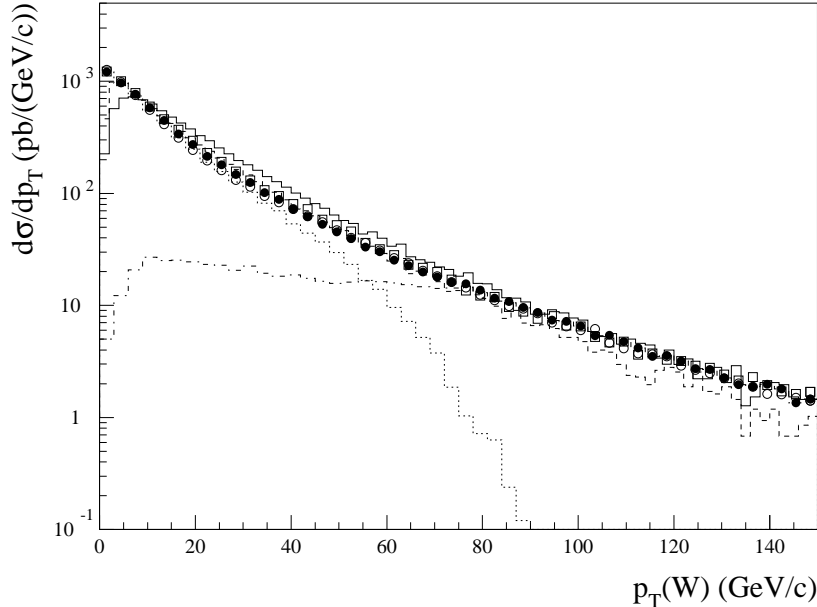


Fig. 5. Tree-level summation of the $W + 0$ jet simulation and the LLL-subtracted $W + 1$ jet simulation for the LHC condition using the PS with the "old" PYTHIA-PS kinematics model. The $W + 0$ jet result for the energy-scale choice of $\mu_F = m_W$ is shown with a dotted histogram, the $W + 1$ jet with a dot-dashed histogram, and the sum is plotted with filled circles. The summed results for $\mu_F = 0.5m_W$ and $\mu_F = 1.5m_W$ are plotted with open circles and open squares, respectively, in order to show the stability against the μ_F variation. The dashed and solid histograms show the ME-corrected PYTHIA predictions for the W production using the "old" and "new" PS models, respectively.

$= 0$, $\text{MSTP}(81) = 0$ and $\text{MSTP}(111) = 0$; *i.e.*, the ME-correction, final-state PS, multiple-interaction and hadronization are turned off. The PDF choice is the default; namely, CTEQ5L is used, too. We can see a good agreement between these two simulations. Any difference in a very low p_T region (< 10 GeV/ c) should be ignored because our Q_0 is relatively large and no intrinsic p_T is considered. In the figure, PYTHIA predictions with the ME correction ($\text{MSTP}(68) = 3$) [13] using the "old" PS ($\text{MSTP}(81) = 0$) and the "new" PS ($\text{MSTP}(81) = 20$) are also illustrated for a reference.

The inclusive W simulation result is also shown with a dotted histogram in Fig. 5 together with the result of the LLL subtracted $W + 1$ jet simulation (dot-dashed histogram) described in the previous section, with the same energy-scale choice of $\mu_F = m_W$. The PS is also applied to the $W + 1$ jet simulation with a PS veto, where the PS is retried if the maximum p_T of the PS branches exceeds the p_T of the $W + 1$ jet ME. The sum of these results is plotted with filled circles. We can see a smooth transition between the two simulations. As described in the previous section, the summed cross section shows good stability against the variation of μ_F . A similar stability should also be observed in this p_T spectrum if the applied PS kinematics shows a good matching to the ME calculation.

The open circles and open squares in Fig. 5 show the summed results for other energy-scale choices of $\mu_F = 0.5m_W$ and $\mu_F = 1.5m_W$, respectively. We can see good stability. Though it is not shown in the figure, the result for $\mu_F = 2.0m_W$ shows a visible discrepancy from these results. This is reasonable since the PS is constructed on the basis of a theory and a model relevant to soft radiations. The underlying approximations may become inappropriate for hard radiations where the hardness (*e.g.*, p_T) is comparable to or larger than the typical energy scale of the considered hard interaction, m_W in the present case. The contribution of such hard radiations may become significant if we set μ_F to be larger than m_W . The energy scale μ_F should not be set very large in our method.

Although the resultant simulation is self-consistent, the summed p_T spectrum seems to be rather soft in low to medium p_T regions (< 50 GeV/ c) compared to the ME-corrected simulations of PYTHIA. This is because the applied PS is soft, as we can see in Fig. 4(a). Though this may be reasonable, we try to construct another kinematics model giving a harder spectrum in the next section.

It may be worth noting here that the two ME-corrected PYTHIA simulations disagree with each other, as we can see in Figs. 4 and 5. The simulation with the "new" PS is harder and in good agreement with our simulation in the high- p_T region. Since the high- p_T spectrum is predominantly determined by the unambiguous $W + 1$ jet ME in our simulation, the "new" PS simulation must be reasonable. The softness of the "old" PS simulation that we see here may also be related to its basic property, which is discussed in the next section.

4 p_T -prefixed kinematics

As we have shown in a previous report [9], the kinematics of the "old" PYTHIA-PS leads to the relation

$$p_T^2 = (1 - z)^2 Q^2 \quad (13)$$

in each branch at the soft limit. As we can see in Eq. (1), the Sudakov form factor becomes smaller if we choose a smaller value for the unphysical parameter, ϵ . This means that the number of parton branches increases. Thus, if we make ϵ sufficiently small, the Q^2 step of the PS evolution becomes nearly continuous compared to the energy scale of the hard interaction. However, the increased branches are predominantly very soft ($z \sim 1$) and do not affect physical properties, such as the p_T of W bosons and visible jets. The above relation can be obtained at this continuous limit; *i.e.*, $p_1^2 \rightarrow p_3^2 = -Q^2$ using the notation in Fig. (3).

On the other hand, ordinary discussions concerning the branching kinematics give us a different relation,

$$p_T^2 = (1 - z)Q^2. \quad (14)$$

This relation can be obtained by assuming that the incoming partons and the radiation are all massless; *i.e.* $p_1^2 = p_2^2 = p_4^2 = 0$. Apparently Eq. (13) gives smaller p_T values than Eq. (14) since $z < 1$. In ME calculations, all initial- and final-state partons are necessarily on-shell; namely, they are nearly massless. Therefore, if we want to achieve a good matching between the PS radiation and the ME radiation, the relation (14) must be better than (13). We test such a model leading to the relation (14) in this section.

Although there may be some sophisticated models, here we adopt a straightforward way to realize this relation. We prefix the p_T of each branch according to Eq. (14) as a starting assumption for calculating the branching kinematics. We keep the definition of z , Eq. (12), since otherwise we would need to apply undesirable energy/momentum corrections in the connection to ME. As a result, we have to abandon relation (11). The p^2 of the evolving partons is derived from energy-momentum conservation conditions. This must not be troublesome, since the virtuality is not a direct observable and the Q^2 of the evolution is not a physically well-defined quantity, as we have already discussed. In the actual implementation, it sometimes happens that the prefixed p_T exceeds the kinematically allowed maximum. We decrease the p_T value to the allowed maximum in such cases.

The filled circles in Fig. 4(b) show the result of a simulation with this new PS kinematics. The evolution to give Q^2 and z is the same as in the previous simulation. Apparently it gives a harder p_T spectrum of W bosons. It should be noted here that relations (13) and (14) are obtained at the soft limit ($Q^2 \ll \hat{s}$). It is not trivial that the difference between these two relations is directly reflected in the visible p_T spectrum of W bosons. For a confirmation, we have tried another simulation with the p_T -prefixed PS kinematics model, in which Eq. (13) is assumed instead of Eq. (14). The result is shown by the open triangles in Fig. 4(a). It is in good agreement with the previous result, confirming that the "old" PYTHIA-PS kinematics actually results in relation (13) and the difference in the PS property at the soft limit is reflected in the visible p_T spectrum of W bosons.

The matching test is retried using the new p_T -prefixed PS in Fig. 6. The simulation conditions are the same as those giving the results in Fig. 5, except for the PS kinematics. We can see a smooth transition between the $W + 0$ jet and $W + 1$ jet simulations again. The spectrum in low to medium p_T regions has become harder and come closer to the PYTHIA simulations with the ME correction. The μ_F dependence is small, but has become larger as we can see in the figure. This must be simply due to the fact that this new PS generates harder radiations. The approximation may become worse, as we have discussed in the previous section. It is, however, possible to evaluate the internal ambiguity by comparing the predictions with different μ_F values; for instance, those with $\mu_F = m_W$ and $\mu_F = 0.5m_W$. In general, a Sudakov suppression has to be applied in order to take higher-order effects into account, if we choose an energy scale apart from the typical energy scale of the considered hard interaction. The suppression is however a few percent and can be ignored for $\mu_F = 0.5m_W$.

It should be noted here again that the Bjorken's x for the hard interaction is given by PS in our method. The PS veto, therefore, alters the PDF for the $W + 1$ jet simulation. The cross section prediction slightly

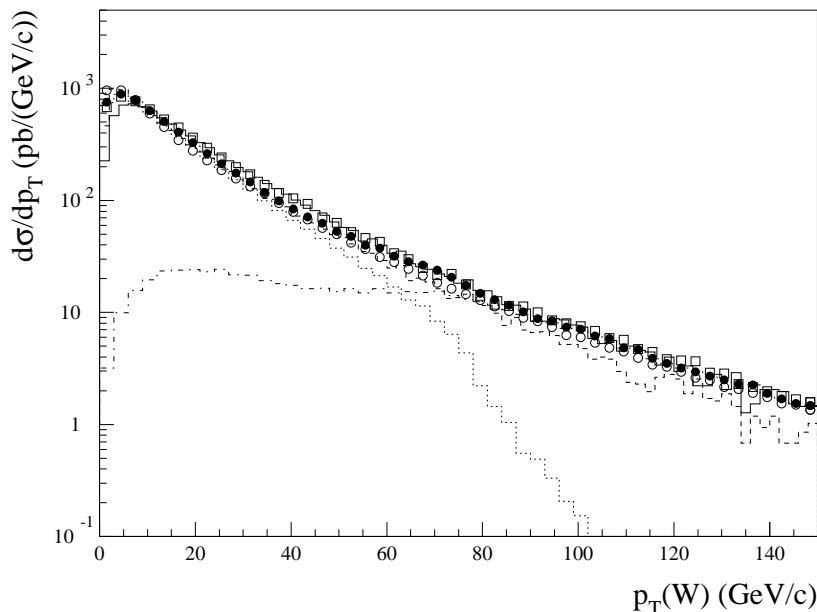


Fig. 6. Tree-level summation of the $W + 0$ jet simulation and the LLL-subtracted $W + 1$ jet simulation for the LHC condition using the p_T -prefixed PS kinematics model. The $W + 0$ jet result for the energy-scale choice of $\mu_F = m_W$ is shown with a dotted histogram, the $W + 1$ jet with a dot-dashed histogram, and the sum with filled circles. The summed results for $\mu_F = 0.5m_W$ and $\mu_F = 1.5m_W$ are plotted with open circles and open squares, respectively. The dashed and solid histograms show the ME-corrected PYTHIA predictions for the W production using the "old" and "new" PS models, respectively.

changes as a result. The filled triangles in Fig. 2 show the results of a simulation with the p_T -prefixed PS assuming the relation (14). At present we have no idea about the question whether this alternation is reasonable or not.

In the course of the present study, we have found that the "new" p_T -ordered PS of PYTHIA shows a behavior quite similar to our p_T -prefixed PS. The result of the "new" PYTHIA-PS simulation without the ME correction is over-plotted in Fig. 4(b) with open circles. We can see that the p_T spectrum is almost identical to our new result.

5 Conclusion

In the limited leading-log (LLL) subtraction method for NLO event generators, the parton shower (PS) to be applied to non-radiative processes must well reproduce the leading-log (LL) contributions in the matrix-element (ME) evaluation of radiative processes. The PS activity depends on the applied model for branching kinematics. We have introduced two kinematics models to be applied to our simple initial-state leading-log PS: a model similar to the "old" PYTHIA-PS and a p_T -prefixed model with a p_T definition motivated by ME calculations. The former shows a behavior similar to the "old" PYTHIA-PS, and the latter results in harder transverse activities, as we expected. We also found that the "new" PYTHIA-PS is similar to the latter.

PS simulations employing these two models have been tested using the W -boson production at LHC as an example. Both simulations show a smooth matching to the LLL subtracted $W + 1$ jet simulation in the p_T distribution of W bosons, though the p_T -prefixed PS results in an apparently harder p_T spectrum than the PS with the "old" PYTHIA kinematics. The summed p_T spectra are stable against the variation of the factorization-scale choice in both simulations. This is a remarkable feature of the LLL subtraction method. The remaining instability can be used as a measure of the internal ambiguity of this method.

The present study is not enough to decide which model is better for our application. The decision must be postponed until further studies can be conducted employing a comparison with experimental

data, such as the Z -boson production data at Tevatron. Lower Q^2 effects that are absent from the present simulations has to be taken into account there.

The method tested in this paper is not dedicated to W -boson production, but can be applied to other processes. Of course, m_W has to be replaced with their *typical* energy scales in such applications. At present, our method is limited to applications to the initial-state radiation. It will, however, be easy to extend it to the final state since the concept is very simple. Once extended, it will allow us to construct NLO event generators for those processes including jet(s) in the final state, which the existing NLO event generator [3] has not yet supported. Even if loop corrections necessary for NLO calculations are absent, our subtraction method will give us a consistent way to simulate multi-jet production processes at the tree level. This will be an alternative to the CKKW method [14].

Acknowledgments

This work has been carried out as an activity of the NLO Working Group, a collaboration between the Japanese ATLAS group and the numerical analysis group (Minami-Tateya group) at KEK. The authors wish to acknowledge useful discussions with the members: J. Kodaira, J. Fujimoto, T. Kaneko and T. Ishikawa of KEK, and K. Kato of Kogakuin University.

References

1. S. Catani and M.H. Seymour, Nucl. Phys. B **485**, 291 (1997);
S. Catani, S. Dittmaier, M.H. Seymour and Z. Trócsányi, Nucl. Phys. B **627**, 189 (2002)
2. J. Collins, J. High Energy Phys. **05**, 004 (2000);
Y. Chen, J. Collins and N. Tkachuk, J. High Energy Phys. **06**, 015 (2001);
Y. Chen, J. Collins and X. Zu, J. High Energy Phys. **04**, 041 (2002)
3. S. Frixione and B.R. Webber, J. High Energy Phys. **06**, 029 (2002)
4. G. Corcella *et al.*, J. High Energy Phys. **01**, 010 (2001)
5. P. Nason and G. Ridolfi, J. High Energy Phys. **08**, 077 (2006)
6. Y. Kurihara, J. Fujimoto, T. Ishikawa, K. Kato, S. Kawabata, T. Munehisa and H. Tanaka, Nucl. Phys. B **654**, 301 (2003)
7. T. Ishikawa, T. Kaneko, K. Kato, S. Kawabata, Y. Shimizu and H. Tanaka, KEK Report 92-19 (1993)
8. S. Kawabata, Comput. Phys. Commun. **41**, 127 (1986); *ibid.*, **88**, 309 (1995); private communication for the treatment of negative cross sections
9. S. Odaka, hep-ph/0604240
10. H.L. Lai *et al.*, Eur. Phys. J. C **12**, 375 (2000)
11. T. Sjöstrand, S. Mrenna and P. Skands, J. High Energy Phys. **05**, 026 (2006)
12. T. Sjöstrand, Phys. Lett. **157B**, 321 (1985);
M. Bengtsson, T. Sjöstrand and M. van Zijl, Z. Physik C **32**, 67 (1986)
13. G. Miu and T. Sjöstrand, Phys. Lett. B **449**, 313 (1999)
14. S. Catani, F. Krauss, R. Kuhn and B.R. Webber, J. High Energy Phys. **11**, 063 (2001)